Supporting Information

Negative dissipation gradients in hysteretic materials

Miriam Jaafar[a†], Óscar Iglesias-Freire[a,b†], Pedro García-Mochales[c], Juan José Sáenz[d,e*] and Agustina Asenjo[a*]

Dissipation in Scanning Force Microscopy

A very intuitive formula deduced by *Cleveland* and co-workers[1] is commonly used to calculate the energy dissipated in scanning force experiments, relying on the fact that, in equilibrium, the average rate at which energy is fed into the cantilever must equal the average rate at which energy is dissipated by the cantilever and the interacting tip. The resulting dissipation of energy associated to tip-sample interactions reads:

$$\langle P_{tip} \rangle = \frac{1}{2} \cdot \frac{k \cdot A^2 \cdot \omega}{Q} \cdot \left[Q \cdot \frac{A_{driver}}{\mathrm{A}} \cdot \sin(\phi) - \frac{\omega}{\omega_0} \right] \qquad \textbf{(E1)}$$

It is important to note that the reason that Q and ω_0 appear in equation **E1** is to express the viscous damping coefficient *b* in terms of experimentally accessible quantities. It does not imply that neither the resonant frequency nor the quality factor of the interacting cantilever remain the same, it only assumes that the viscous damping coefficient describing the damping of the body of the lever remains unchanged. In the amplitude modulation mode, topography imaging is performed with the amplitude held constant by the main feedback loop. If a *PLL* is implemented, another feedback loop tracks the resonance peak by setting $\phi = {}^{\pi}/_{2}$, so that the free amplitude of the cantilever turns out to be $A_0 = Q \cdot A_{drive}$. With all this:

$$\langle P_{tip} \rangle = \frac{1}{2} \cdot \frac{k \cdot A^2 \cdot \omega}{Q} \cdot \left[\frac{A_0}{\mathrm{A}} - \frac{\omega}{\omega_0} \right] \qquad \textbf{(E2)}$$

An important consequence of former equation is that non-dissipative interactions connect changes in the resonance frequency to variations in the oscillation amplitude, in such a way that attractive forces “soften” the cantilever and give rise to larger amplitudes and vizeversa, for constant excitation signals as is usually the case in *AM-AFM*. Hence, during the topographic scan – and disregarding eventual errors in the main feedback – one can associate variations in the oscillation frequency to dissipative processes. Therefore, during the retrace scan in *MFM* measurements one would expect changes in the oscillation amplitude due to non-dissipative magnetostatic interactions. However, such variations are predicted to be very small and strong frequency shifts are usually necessary to register this effect. For instance, for a cantilever with a free resonance frequency ω_0=70 kHz and a free oscillation amplitude A_0=10 nm, frequency shifts of 100 Hz result in an amplitude change of 15 pm, below the thermal noise level at room temperature.

Micromagnetic simulations

Simulations were performed with the *OOMMF* free-source code, (available at http://math.nist.gov/oommf), using the *3D Oxsii* mode and (3x3x3) nm^3 cubic cells. The tip was modeled as a square based pyramid coated with a 51 nm thick cobalt layer, with a saturation magnetization M_S=1.4·10^6 A/m, a magnetocrystalline anisotropy K_1=5.3·10^5 J/m^3 and an exchange stiffness A=3.0 10^{-11} J/m. The sample was simulated as a 36 nm thick film and its magnetization was kept fixed during the simulation (M_S^{sample}=3.3·10^5 A/m), either parallel or antiparallel to the magnetization in the tip.

To simulate the tip oscillation, the tip apex was initially located in the center of the domain (138 nm in width) and 21 nm above the sample surface, moved down to a tip-sample separation of 9 nm in 3 nm steps and, then, it was retracted back to the initial position. In the initial magnetic configuration of the tip, all spins are pointing downwards and in every step the magnetization is fully relaxed before moving the tip; this final magnetization being the starting configuration for the next step. The approach-retract cycle was repeated twice, but only the second one was used in order to avoid 'memory' effects of the initial magnetic configuration. The tip magnetization presents a hysteretic behavior and so does the magnetic force between the two objects. Let us label the Z component of the magnetic force during the approach and retract curves, at a given separation distance, as $F_{z,\downarrow}$ and $F_{z,\uparrow}$, respectively. Deviations of the force from the average value during the second cycle ($\Delta F_{z,\downarrow}=F_{z,\downarrow}-\langle F_z\rangle$ and $\Delta F_{z,\uparrow}=F_{z,\uparrow}-\langle F_z\rangle$) are depicted in Supplementary Figure 1c-d for both cases, where the average force is $\langle F_z\rangle=(F_{z,\downarrow}+F_{z,\uparrow})/2$.

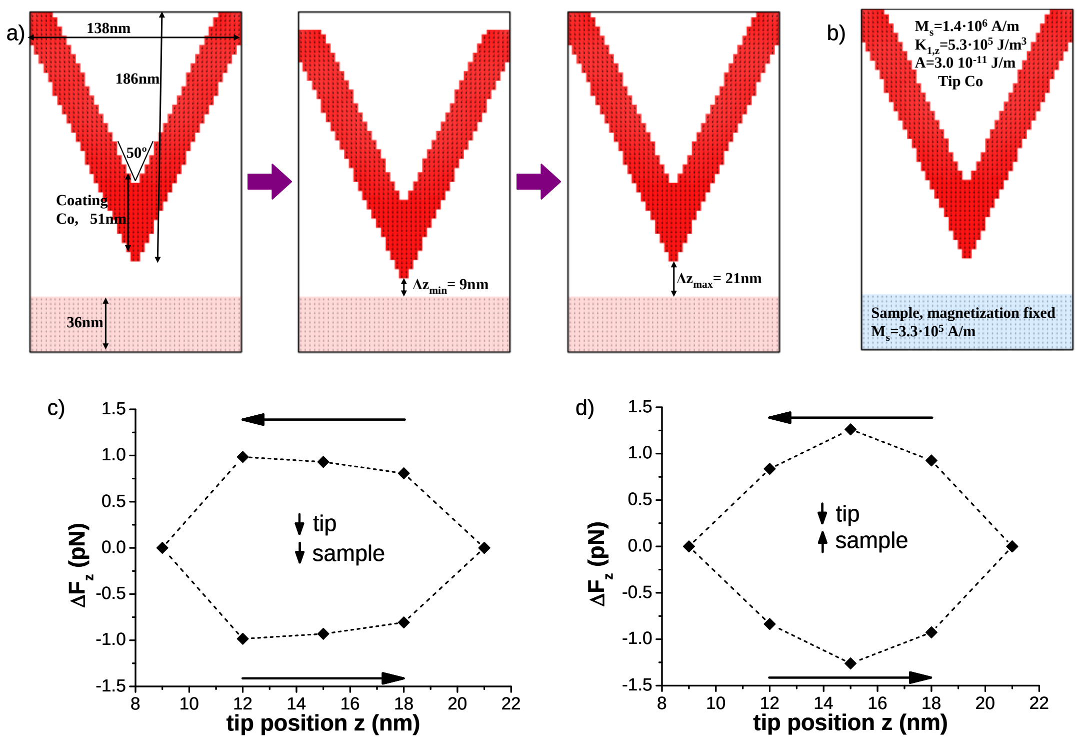

Supplementary Figure 1: **Micromagnetic simulations.** (a)-(b) Sketch of the tip-sample configuration used in the calculations for (a) attractive and (b) repulsive interactions. (c)-(d) Hysteresis loops in the tip-sample force as function of the separation distance during one oscillation cycle, obtained for the (c) parallel and (d) antiparallel configurations.

Additional MFM and dissipation measurements

Additional measurements were performed varying the MFM probes, the samples, the experimental conditions and the operation mode.

Topography	MFM signal	Dissipation
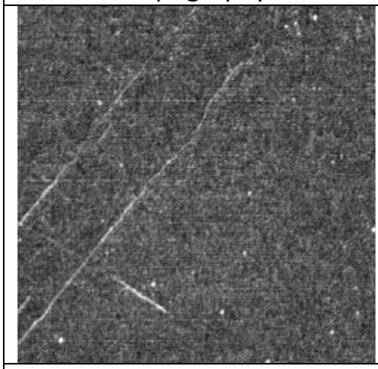	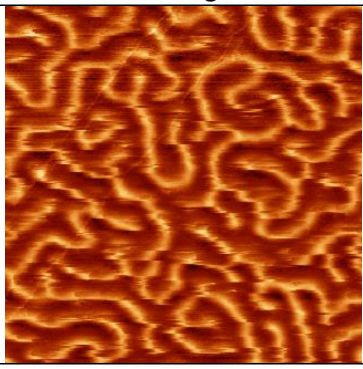	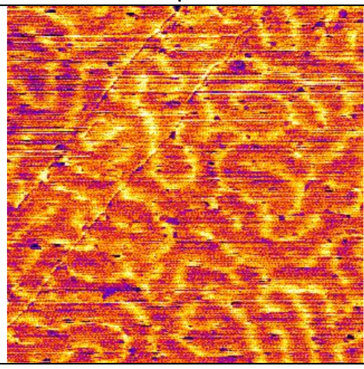

Supplementary Figure 2: Topography, MFM signal and Dissipation map of a CoPt thin film. The images are obtained in standard two passes operation mode (topography in Amplitude Modulation) with PLL feedback activated by using a *Budget Sensors* Probe. Ambient conditions.
Images size 3.4µm x 3.4µm

Topography	MFM signal	Dissipation
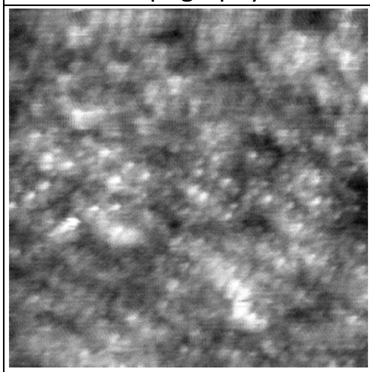		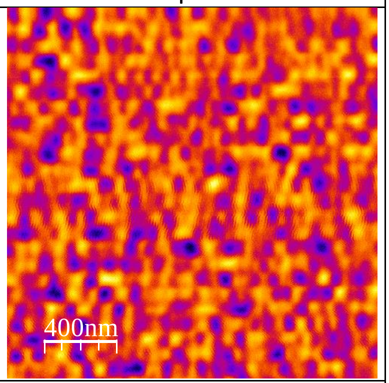

Supplementary Figure 3: Topography, MFM signal and Dissipation map of a high density hard disk. The images are obtained in standard two passes operation mode (topography in Amplitude Modulation) with PLL feedback activated by using a *home-coated* probe[2]. Ambient conditions.
Images size 2 µm x 2 µm

Topography	MFM signal	Dissipation
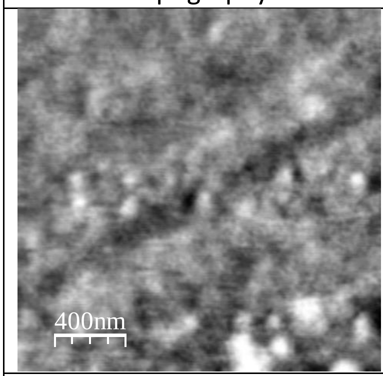	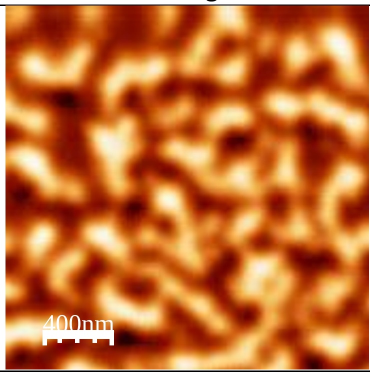	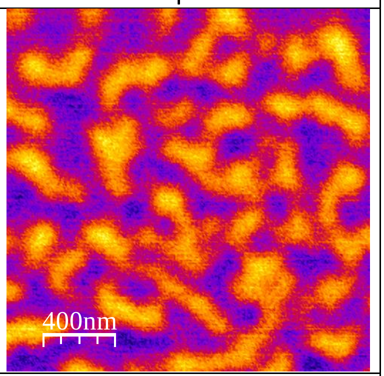

Supplementary Figure 4: Topography, MFM signal and Dissipation map of a CoNi sample. The images are obtained in two passes operation mode (topography in Drive Amplitude Modulation[3]) with PLL feedback. Ambient conditions. *Nanosensors PPP- MFMR* probe. Images size 2 µm x 2 µm

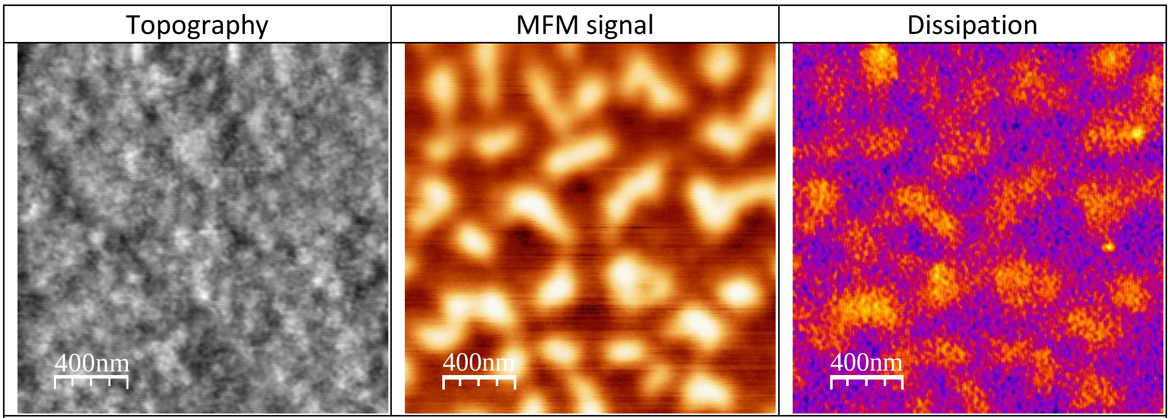

Supplementary Figure 5: Topography, MFM signal and Dissipation map of a CoNi sample. The images are obtained in two passes operation mode (topography in Drive Amplitude Modulation) with PLL feedback. High Vacuum environment. *Nanosensors PPP- MFMR* probe. Images size 2 µm x 2 µm

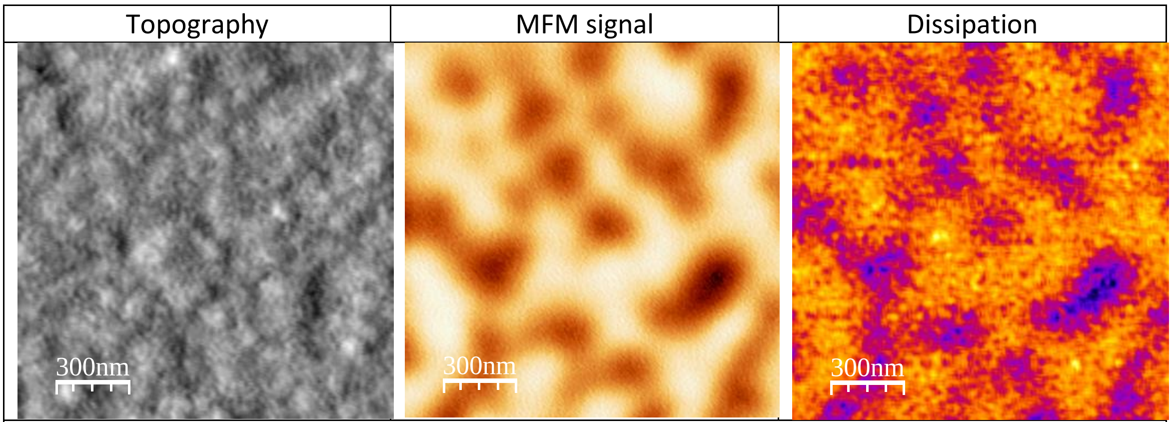

Supplementary Figure 6: Topography, MFM signal and Dissipation map of a CoNi sample. The images are obtained in standard two passes operation mode (topography in Frequency Modulation i.e. with PLL feedback). Ambient conditions. *Nanosensors PPP- MFMR* probe. Images size 1.5 µm x 1.5 µm

Acknowledgements

I. Lucas, P. Strichovanec for the CoPt thin film sample

References

[1] J. P.Cleveland, B. Anczykowski, A. E. Schmid, V. B. Elings, *Appl. Phys. Lett*., 1998, **72**, 2613.
[2] O. Iglesias Freire et al. *Beilstein J. Nanotechnol*. 2016, **7**, 1068–1074.
[3] M. Jaafar et al. *Beilstein J. Nanotechnol*. 2012, **3**, 336–344